Improvement of antimicrobial activity of quinazolinone derivatives by loading into chitosan/TPP nanoparticles.

Nehal Salahuddin*, Ahmed A. Elbarbary, Hend A. Alkabes

Department of Chemistry, Faculty of Science, Tanta University, Tanta 31527, Egypt

Abstract- Chitosan (CS)/Quinazolinone/Tripolyphosphate (TPP) nanoparticles have been synthesized using 2.3:1 molar ratio of CS/TPP in presence of quinazolinone derivatives (I-IV) through simple one step reaction. The mixture was subjected to ultrasonic waves to obtain the nanoparticles. The nanoparticles are quite uniform in size, spherical shape and rod like structure depending on the quinazolinone derivatives. The amount of loaded quinazolinone was calculated using UV-Vis spectrophotometer and TGA. The release of quinazolinone derivatives (I-IV) in acidic medium (pH=2) is significantly higher than in slightly acidic medium (pH=6.8). The proposed mechanism based on zero orders, first order, Higuchi, Hixson-Crowell and Korsmeyer-Peppas model equation are explored. The antimicrobial activity of nanoparticles was investigated against Escherichia coli, Pseudomonas aeruginosa, Staphylococcus epidermis and Staphylococcus aureas.

Index Terms- Chitosan, tripolyphosphate, nanoparticles, quinazolinone derivatives, antimicrobial activity.

I. INTRODUCTION

Quinazolinone derivatives possess versatile type of biological activities such as antibacterial, antifungal, analgesic, anti-inflammatory, anthelminthic, anticonvulsant, anti HIV, anti-tubercular, CNS depressant, cytotoxicity and diuretic [1, 2] Search for sustained form of these quinazolinone derivatives was necessitated by the need firstly to improve compliance by patients, thereby minimizing the development of microbial resistance and secondly to reduce the frequency of administration thus contributing to minimize the extensive side effects associated with the quinazolinone derivatives.

Polymeric nanoparticles have been used increasingly in various fields such as drug delivery, imaging and tissue engineering. The main reason justifying the wide spread use of polymeric nanoparticles relies on the displayed high surface to volume ratio that improves the loading capacity of the selected molecule. In addition, increased drug absorption might be attained by the capacity of nanoparticles to reduce epithelial resistance to transport [3-5].

Recently, polymeric nanoparticles prepared from biocompatible and biodegradable polymers are used in drug delivery to increase the drug safety in which the drug is entrapped, encapsulated or attached to the nanoparticle matrix [6]. Depending on the preparation methods, there are two morphologies of nanoparticles: nanospheres and nanocapsules [7, 8]. Nanospheres have monolithic type structure in which drugs are adsorbed on their surfaces. Nanocapsules are systems in which exhibit a membrane- wall structure and the drugs are entrapped in the core or adsorbed onto their exterior surface.

Chitosan (CS) is cationic polysaccharide composed of repeating units of N-acetyl glucosamine and D-glucosamine that are β-(1→4)-linked. CS has excellent biodegradable, biocompatible, unique polymeric cationic character, film forming properties, non-toxicity and antimicrobial activity. It has been examined extensively in the pharmaceutical industry for its potential in the development of drug delivery system [9].

CS derivatives formed by N–substitution with carboxyl bearing group showed improvement of solubility in aqueous media and zwitterion character. This allows the formation of clear gels at neutral and alkaline pH media however, promotes accumulation in acidic pH environment. This accumulation behavior led to the need to crosslink the CS molecules to overcome this problem and to stabilize CS in acidic media. CS microparticles cross linked with glutraldehyde were shown to be long- acting biodegradable carriers suitable for use in microparticles delivery system [10-12]. In order to surmount the toxicity problems associated with chemical crosslinking with glutaraldehyde and epichlorohydrin, ionic crosslinking has been utilized in the production of chitosan tri polyphosphate (CS/TPP) microparticles. Drug release from CS based particulate systems depends upon the extent of crosslinking, morphology, size and density of the particulate system.

The objective of this work was directed to produce CS/Quinazolinone nanoparticles including in the formulation TPP as crosslinking agent using ultrasonic waves with CS/TPP 2.3:1 molar ratio and to evaluate the effect of quinazolinone derivatives on morphology of CSTPP nanoparticles, loading efficiency and release rate. In addition, antimicrobial activity of quinazolinone derivatives nanoparticles was discussed.

II. MATERIALS AND METHODS

CS (Across organics, USA, Mw. 100,000-300,000 deacetylation degree (DD) 90%), sodium tripolyphoshste (TPP) (Across organics, USA), dimethylsulfoxide (DMSO) (Sigma-Aldrich), Hydrazine mono hydrate (Laboratory rasayan), concentrated hydrochloric acid (HCl) (Adwic, Egypt), monosodium phosphate (Adwic, Egypt), disodium phosphate (Adwic, Egypt), Nutrient agar (Alpha chemicke), anthranilic acid (Lobachemia), benzoyl chloride (Panreac, Espana), pyridine (Adwic, Egypt), bromine water (Aldrich), acetic acid (Adwic, Egypt), Para-chlorobenzoylchloride (Merck, Sohuchardt) were purchased and used as received. All melting points (m.p.) were uncorrected.

Preparation of 2-phenyl-4(3H)-3, 1-benzoxazinone

To a stirred solution of anthranilic acid (0.05 mol) in pyridine (60 ml), benzoyl chloride (0.05 mol) was added, the temperature was adjusted to be 0-5 °C. The reaction mixture was stirred for 2 h at r.t. untill a solid product was formed. This was precipitated pale yellow solid and filtered (yield 83 %, m. p. 113 °C) [1]. The same procedure was done for preparing 6,8-dibromo-2-phenyl-4(3H)-3,1-benzoxazinone, 6-bromo-2- phenyl–4(3H)-3,1-benzoxazinone and 2-(4-chloro phenyl)-4(3H)-3,1-benzoxazinone.

Preparation of 3-amino-2- phenyl-4(3H)-quinazolinone (I)

To a stirred solution of 2- phenyl -4(3H)-3,1-benzoxazinone (0.05 mol) in pyridine (20 ml), 80% $N_2H_4.H_2O$ (0.15 mol) was added. The reaction mixture was stirred and refluxed for 20 minutes. The crude product was filtered off and recrystallized from ethanol to afford a white solid, (yield 88%, m.p. 177-178 °C) [1]. The same procedure was done to prepare 6, 8-dibromo-2- phenyl -4(3H)-quinazolinone (II) (yield 65%, m.p. 228-234 °C) [1], 6-bromo-2- phenyl–4(3H)–quinazolinone (III) (yield 76%, m.p. 160-164 °C) and 3-amino-2-(4-chloro phenyl)-4(3H)-quinazolinone (IV) (yield 40%, m.p. 166-168 °C) [13].

Preparation of CSTPP nanoparticle

CS nanoparticles were prepared by ionotropic gelation of CS in the presence of TPP using (2.3:1) molar ratio. TPP (1 g dissolved in distilled water) was added to CS solution (1 g dissolved in 100 ml of 1% acetic acid) during sonication for 15 minutes at 30 °C and stirred for 45 minutes, CSTPP nanoparticles were centrifuged, the supernatant was discarded and the deposit was re-dispersed in distilled water three times, recentrifuged and dried at 40 °C.

Preparation of CS-Quinazolinone–TPP nanoparticle

0.0011 mol of quinazolinone derivatives (I-IV) was added to CS solution (1 g was dissolved in 80 ml of 1% acetic acid) and stirred for 30 minutes. Then TPP (1 g dissolved in distilled water) was added during sonication for 15 minutes followed by stirring for 2 h then, the products were separated using centrifuge and dried at 40 °C.

Preparation of buffer solution

Phosphate buffer solutions (PB) were prepared by dissolving dibasic sodium phosphate (44 g) in 600 ml deionized water and monobasic sodium phosphate (22 g) in 400 ml deionized water followed by drop wise addition of monobasic solution to dibasic solution until pH was adjusted at 6.8. For pH=2, drops of (0.8 M) HCl were added to deionized water until pH adjusted to 2.

Release Measurements

10 mg samples suspended in 1 ml buffer were transferred into a dialysis bag with a cut-off molecular weight of 35 KDa. The dialysis bag was then suspended in 100 ml of PB (pH=6.8) and HCl solution (pH=2). At specific intervals, 3ml of the buffer was collected from the release medium to determine the concentration of quinazolinone derivatives by UV-Vis spectrophotometer.

Adsorption experiment

The amount of loaded quinazolinone derivatives on nanoparticles was determined by measuring the absorbance of the solution using the UV-Vis spectrophotometer at λ_{max}=230, 242, 231, 233 nm for I, II, III and IV, respectively. The loading efficiency is calculated according to the following equation

$$\%\ \text{Efficiency} = \left(\frac{W_a}{W_t}\right) \times 100 \qquad (1)$$

Where W_a is the actual content of quinazolinone and W_t is the initial content of quinazolinone. It was found to be 65%, 74.9%, 61% and 46.9% for CSTPPI, CSTPPII, CSTPPIII and CSTPPIV, respectively.

***In vitro* release kinetics**

The data obtained from in-vitro release studies were analyzed by fitting to various kinetics equations to study the mechanism of quinazolinone derivatives release from prepared formulations [14-18]. The kinetic models are formulated in the following equations.

Zero-order release kinetics:

Where W is the cumulative drug release percent during time t, $W_\circ$ is the cumulative drug release at t= 0 and $k_\circ$ is zero-order drug release rate constant.

$$W = W_\circ + k_\circ t \quad (2)$$

First-order release kinetics: $\log(100 - W) = \log 100 - k_1 t \quad (3)$

Higuchi model: $W = k_H\, t^{1/2} \quad (4)$

Hixson-Crowell Kinetics $(W - 100)^{1/3} = 100^{1/3} - k_{Hix}\, t \quad (5)$

Krosmeryer-Peppas equation $F = \frac{M_t}{M_\infty} = k \times t^n \quad (6)$

Where $k_\circ$, k_1, k_H and k_{Hix} are drug release rate constant of zero order , first order, Higuchi mode and Hixson-Crowell, W is the percent released of drug at time t, F is the fraction release of drug into the dissolution media, k is a constant. Based on the Krosmyer-Peppas equation n is the diffusional exponent, that show the release of drug transport mechanism, values of the n exponent equal to or less than 0.5 were characteristic of Fickian or quasi-Fickian diffusion, whereas values in the range of 0.5 to 1 were an indication of anomalous for drug release or indicate the contribution of non-Fickian processes. On other hand, a unity value for n would be expected for zero order release.

***In vitro* antibacterial Activity**

The bacterial strains were obtained from Bacteriological laboratory of Botany department, Microbiology section, Faculty of science, Tanta University, Egypt. The Gram-negative bacteria (Escherichia coli ATCC 8739, Pseudomonas aeruginosa ATCC 9027) and Gram-positive bacteria (Staphylococcus aureus ATCC 6633, Staphylococcus epidermidis ATCC 12228) were used to examine the antibacterial activity of the nanoparticles. The bacterial strains were maintained on nutrient agar (28 g nutrient agar per liter, pH=7.4). All media were sterilized in autoclave before experiments. 6.5×10^5 CFU were incubated for 24 h.

quinazolinone derivatives (I-IV), CS, CSTPP, and CS/ Quinazolinone/TPP (CSTPPI, CSTPPII, CSTPPIII, CSTPPIV) were screened for their antibacterial activity against the above bacterial strains. The antibacterial activity of the tested samples was determined by well diffusion method. Powder samples of tested compounds (20 mg/ml) were dispersed in DMSO. DMSO was used as negative control. A caliper was used to measure the inhibition zones. Three replicates were carried out. The antibacterial effect of quinazolinone derivatives, CS and quinazolinone loaded nanoparticles on the microorganism was determined by the size of the inhibitory zone after 24 h.

III. RESULTS AND DISCUSSION

Most of the nanoparticles prepared from water insoluble polymers were involved heat, organic solvent or mechanical stirring that can be harmful to the drug stability. In addition some preparation methods are complex and require long time and energy consuming [6]. Furthermore, high crosslinking density leads to lower diffusion of drug from nanoparticles which consequently decrease the burst release and rate of release. CS contains abundant amino and hydroxyl groups which enable particle formulation via physical and chemical crosslinking. Ionic crosslinking of CS is a typical non covalent interaction which can be formed by association of positively charge NH_3^+ of CS in acid medium with negatively charged multivalent ions such as TPP for pharmaceutical application. Physical crosslinking is reversible and may provide non toxicity of the regents however; using covalently bonded crosslinks may provide potential toxicity. Although many efforts have been done to obtain nanoparticles of CSTPP, optimization of fabrication conditions is still important topic in this field. One of the problems in biomaterials for drug delivery and need to overcome is the burst release of encapsulated or entrapped drugs. By controlling the release of drugs, one can not only optimize the therapeutic effects of the drug, but also influence their biological activity. In this study the effect of different heterocyclic quinazolinone derivatives (scheme.1) on the adsorption efficiency of CSTPP nanoparticles was studied using sonication method. The release and antimicrobial activity against Gram-positive and Gram–negative bacteria were evaluated and compared with quinazolinone derivatives.

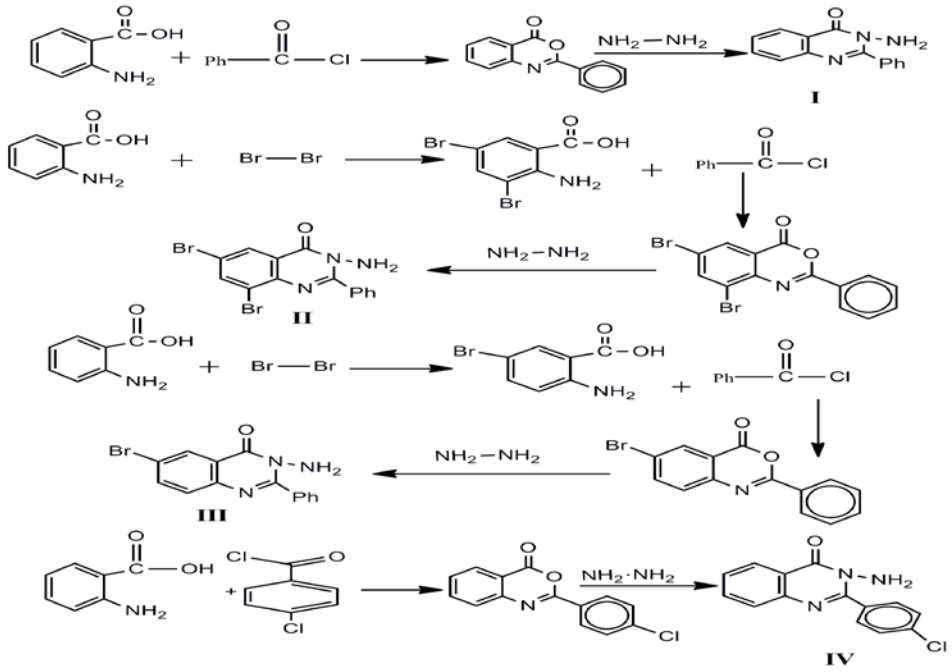

Scheme 1: Preparation of quinazolinone derivatives.

Morphology

The XRD pattern of CS (Fig.1) shows two prominent crystalline peaks at 10˚and 20˚ due to presence of plenty of OH and NH_2 groups that forms strong inter and intra molecular hydrogen bonds [19]. Cross-linking CS by TPP (CSTPP) (Fig.1) reveals disappearance of peak at 10˚, shift of peak at 20˚ to 17.2˚ and a new broader peak at 24.37 ˚ is formed. This could be attributed to the rearrangement of molecules in the crystal lattice. It was reported that after ionic cross-linking CS with TPP, no peak is detected in the diffractgrams of CS nanoparticles, reflecting the destruction of the native CS packing structure [20, 21]. In case of quinazolinone derivatives (I-IV), several diffraction sharp peaks are observed at 8.44˚, 14˚, 16˚, 19˚, 23˚ and 24.5˚ due to crystalline phase of quinazolinone derivatives. Compared to I loaded into CSTPP nanoparticle (CSTPPI) (Fig. 1a), the sharp peaks for compound I was observed at the same positions. This indicates the inclusion of compound I in CSTPP nanoparticles. In addition, the peak for CSTPP at 17˚ was shifted to 18.5˚. The same results were observed in CSTPPII, CSTPPIII and CSTPPIV (Fig.1). This confirms the adsorption of the quinazolinone derivatives on the surface of CSTPP nanoparticles. It was reported that peaks for the plain drug were not seen for the drug loaded microspheres due to the encapsulation of drug in the interpenetrating polymeric network [22]. Crystalline sizes of nanoparticles were estimated using Scherer's equation (7). $$D = \frac{K\lambda}{\beta \cos\theta} \quad (7)$$

Where K=constant (0.89<K<1), λ wavelength of the X-ray λ=0.154 nm, B=FWHM (full width at half maximum width of the diffraction peak, θ = diffraction angle in radian. The highest three peaks were selected for this calculation. The average crystal size was increased by adsorption of quinazolinone from 6 nm in CSTPP to 43, 32.7, 21 and 35.8 nm in CSTPPI, CSTPPII, CSTPPIII and CSTPPIV, respectively.

The morphology of CSTPP nanoparticles was characterized by TEM observations. The TEM image (Fig.2) shows a relatively narrow size distribution of mono dispersed nanoparticles with spheroid morphology with size average of 21 nm and standard deviation (S.D) was ± 5 nm. The size of these nanoparticles is smaller than that determined (>200 nm) previously [23, 24]. It has been reported that CSTPP nanoparticles are rough in shape [24]. TEM image in Fig.2 shows that CSTPPI and CSTPPII nanoparticles have a similar morphology for CSTPP. The average sizes of these nanoparticles are varied according to quinazolinone derivatives from 31 to 41 nm and S.D were ±7, ±8 nm for CSTPPI, CSTPPII, respectively. However, CSTPPIII showed rod like structure with thickness 33 nm and length of 55 nm with S.D ±10 nm. The nanorods have an aspect ratio of 1.6. CSTPPIV shows sphere with rod like structure. The average diameter of spheroid is 27 nm and the rods have thickness of 27 nm and length of 54 nm with S.D ±6 nm. The nanorods have an aspect ratio of 2. The size of nanoparticles measured by TEM is almost consistent with the size estimated from XRD by Scherer equation. The nanoparticles were further visualized by SEM (Fig. 3). A spherical shape is observed for CSTPP with average size of 84 nm and S.D ±7 nm. It is worth noting that CSTPPI (Fig. 3) has a rough shape with mean average diameter of 135 nm with S.D ±18 nm. It is observed that there is consistent increase is the dimensions of CSTPP nanoparticles due to loading of quinazolinone [25, 20]. Kumar et al [26] was reported smooth surface morphologies of CS cross-linked with glutaraldehyde. The surface morphology characteristics have an impact on bioadhesion. It has been found that the nanospheres with a coarser and more porous surface may offer enhanced bioadhesivity as compared to those with a smoother texture. The nanorod CSTPPIII show uniform size over their entire length and some nanorods stick together. SEM image (Fig. 3) confirms that the nanorod has rectangular shape with thickness of 96 nm and length of 131 nm with S.D ±20 nm. The nanorods have an aspect ratio of 1.36. Recently, CS- Insulin- TPP shows presence of granular particles with rod shaped morphology of different sizes whose morphology differed from the CSTPP [27].

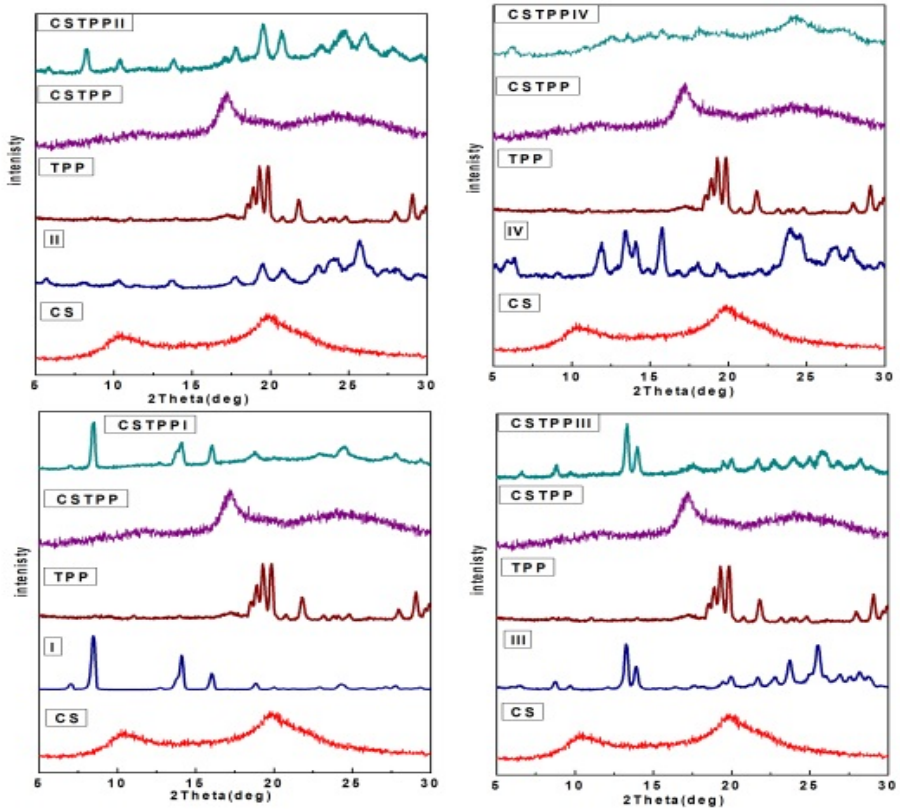

Fig 1: XRD pattern of CS, TPP, I-IV, CSTPP, CSTPPI, CSTPPII, CSTPPIII and CSTPPIV nanoparticles

From SEM and TEM observation, nanoparticles were successfully synthesized and the morphology of the nanoparticles depends on the structure of quinazolinone derivatives.

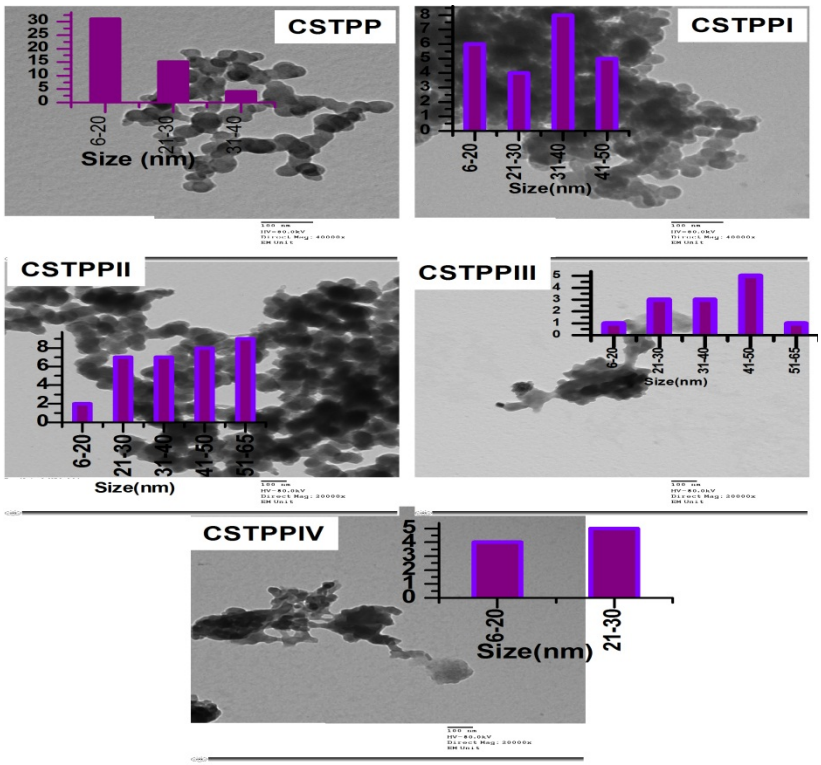

Fig 2: TEM images of CSTPP, CSTPPI, CSTPPII, CSTPPIII and CSTPPIV.

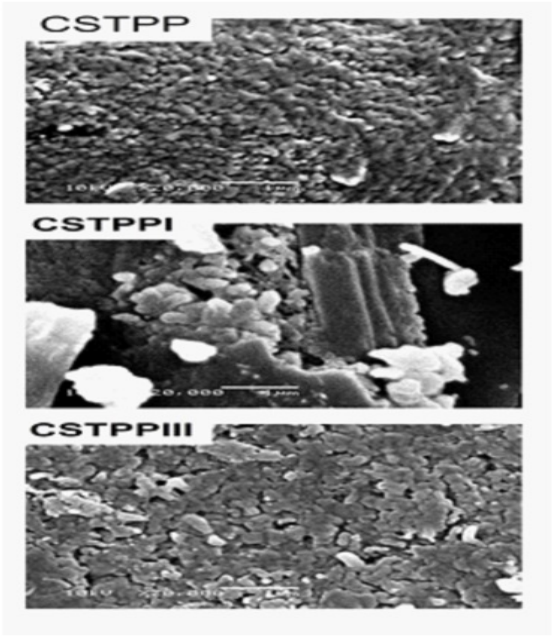

Fig 3: SEM images of CSTPP, CSTPPI and CSTPPIII.

The composition of CS, TPP, quinazolinone derivatives (I-IV), CSTPP and CS-Quinazolinone –TPP was further characterized by FT-IR (Fig. 4). The spectrum of CS displays a strong absorption band at 3437 cm^{-1} due to OH and amine N-H symmetrical stretching vibration. A peak at 2921 cm^{-1} was due to symmetrical C-H stretching vibration attributed to pyranose ring. The sharp peak at 1383 cm^{-1} was assigned to CH_3 in amide group. The broad peak at 1095 cm^{-1} was indicated C-O –C stretching vibration in CS [28], peaks at 1649 and 1425 cm^{-1} were due to C=O stretching (amide I) and N-H stretching (amide II). The absorption band at 1153 cm^{-1} was assigned to the anti-symmetric stretching of C-O-C bridge and 1095 cm^{-1}, 1010 cm^{-1} were assigned to the skeletal vibration involving the C-O stretching. The spectrum of TPP presents absorption bands at 1217, 1143, 1069 and 898 cm^{-1} that were attributed to P-O stretching, symmetric and anti-symmetric stretching vibrations in PO_2 group, symmetric and anti-symmetric stretching vibrations in PO_3 group and anti-symmetric stretching of the P-O-P bridge, respectively [29].

FT-IR spectrum of CSTPP nanoparticles shows absorption band at 1542 cm^{-1} due to NH_3^+ vibration. Moreover, the band at 3437 cm^{-1} and 1649 cm^{-1} related to OH and C=O stretching (amide I) were shifted to 3447 cm^{-1} and 1624 cm^{-1}, implying electrostatic interaction between NH_3^+ groups of CS and phosphoric groups of TPP within the nanoparticles [121, 30, 31].

FT-IR spectrum of I shows bands at 3438, 3309 cm^{-1}, 3209 cm^{-1} corresponding to (N-H), multiple weak absorption peaks over the 3038, 3068 cm^{-1} corresponding to Qu-H and Ar-H stretching vibration absorption peaks, the strong absorption at 1660 cm^{-1}, 1640 cm^{-1}, 1564-1474 cm^{-1} and 765 - 696 cm^{-1} correspond to the C=O stretching Vibration, C=N stretching vibration, (the skeleton vibration of the aryl and heterocyclic ring) and the phenyl-substituted at the 2-position in the quinazolinone, respectively [32]. The same bands of I was observed in II-IV. Moreover, bands at 562, 542, 562 and 539 cm^{-1} related to (C-Br) substituted at the 6, 8-position, (C-Br) substituted at the 6-position and (C-Cl) substituted at 4-phenyl at position -2 for II, III and IV, respectively are observed.

FT-IR spectrum of CSTPPI exhibited similar absorption bands with slight shift at bands 1624, 1542 and 3447 cm^{-1} related to C=O stretching (amide I), NH_3^+ vibration and OH to 1661, 1564 and 3423 cm^{-1}, respectively. Thus confirming the interaction between nanoparticles and quinazolinone derivatives. The peak at 1624 cm^{-1} related to C=O of CSTPP emerged with peak at 1661 cm^{-1} related to C=O of hetero cyclic compound. Similar observation was reported in CSTPPII, CSTPPIII and CSTPPIV. From the above results it is proved that the quinazolinone derivatives are integrated into the nanoparticles and there is an physical interaction between them.

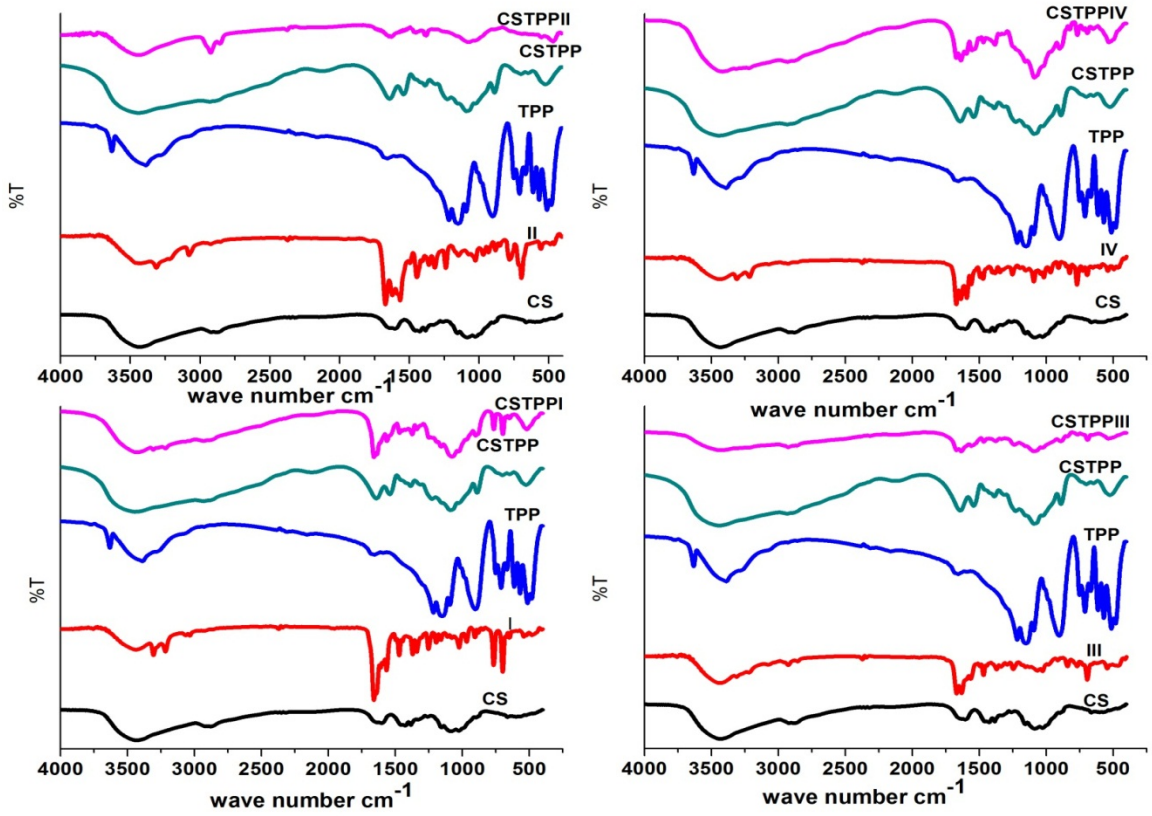

Fig 4: FTIR spectra of CS, TPP, I, II, III, IV, CSTPP, CSTPPI, CSTPPII, CSTPPIII and CSTPPIV.

Thermal properties

TGA and DTGA data of CSTPP are presented in Fig.5a, b. It is seen that weight loss is directly related to increasing the heating temperature. Three steps weight loss are observed from TGA of CS. First step from 50-110 $^{\circ}C$ can be assigned to the release of hydroscopic water molecules. The second weight loss observed from 200-350 $^{\circ}C$ is typical to degradation of saccharide ring while the third weight loss between 575-798 $^{\circ}C$ can be assigned to further degradation and decomposition of acetylated unit of CS. While DTGA shows three peaks at 57.87 $^{\circ}C$, 229.39 °C and 774 $^{\circ}C$ [25].

TGA and DTGA of CSTPPI (Fig.5a, b) show the same characteristic peaks of CSTPP. While second weight loss between 200-350 $^{\circ}C$ in CSTPP is shifted to 200-565 $^{\circ}C$ in TGA and peak at 229 $^{\circ}C$ is shifted to 237.5 $^{\circ}C$ in DTGA. This may be assigned to interaction of CSTPP with quinazolione and decomposition of quinazolinone derivatives. DTGA of CSTPPII, CSTPPIII and CSTPPIV showed the same characteristic peaks of CSTPP with the appearance of new peak at 293 $^{\circ}C$, 270 $^{\circ}C$ and 260 $^{\circ}C$, respectively. This can assigned to the decomposition of quinazolinone derivatives. The weight loss percentage at this temperature range was thus used to compute the amount of loaded quinazolinone derivatives (Table 1).

In vitro release of quinazolinone from nanoparticles

The loading percentage of quinazolinone derivatives in CSTPP was further determined by UV-Vis according to the following equation (3) and summarized in Table1.

Fig.6. displayed the release profile of quinazolinone from CSTPP nanoparticles. The release of quinazolinone derivatives was gradually increased with time in pH=2, 6.8 (Fig. 6). The slow release of I-IV from CSTPP may be due to high percentage of cross linker and steric hindrance in quinazolinone derivatives that delay the release. The release of quinazolinone compound (I-IV) loaded into CSTPP in pH=2 is higher than pH=6.8 (Fig. 6). The release of IV after 55 h was 95% in pH=2 while in pH=6.8 was 45% [33]. Bhumkar et al have reported that CSTPP nanoparticles have higher swelling in pH=2. In another publication the swelling index obtained for cross-linked chitosan at pH=3 (668.85%) was distinctly higher than the (157.65%) obtained for cross-linked chitosan at pH=9 [33]. In the acidic medium, the quinazolinone derivatives rate is relatively rapid in comparison with a slightly acidic buffer solution which attributed to the electrostatic repulsion mechanism that lead to increase intra particle spaces in the nanoparticles, results from the protonated amine (NH_3^+). In contrast to the pH= 6.8 buffer solution, NH_2 groups of CS and quinazolinone mainly attach to the surface of the nanoparticles so slow down release rate of the quinazolinone derivatives in pH 6.8. Large surface area available for dissolution with a small particle size, (CSTPPIV) favor rapid release of the quinazolinone compared to larger nanospheres (CSTPPII) [34].

Zhou et al [35] reported that the release of drugs from micro spheres involves two different mechanisms of drug molecules diffusion and polymer matrix degradation. The burst release of drug is associated with those drug molecules dispersing close to the microsphere surface, which easily diffuse in the initial incubation time. This hypothesis was suitable for ammonium glycyrrhizinate release from CS [36]. This was attributed to diffusion of drug through the pores or on the surface of nanoparticles in a short time. In addition nanoparticles with huge specific surface area can adsorb drug so the burst release is due to desorption of the drug from nanoparticle surface. The burst release in the first 0.5 h of BSA was observed to be ranged from 85.3% to 87.9% depending on the loading capacity due to the poor interaction between them that favor the desorption at ionic environment [37].

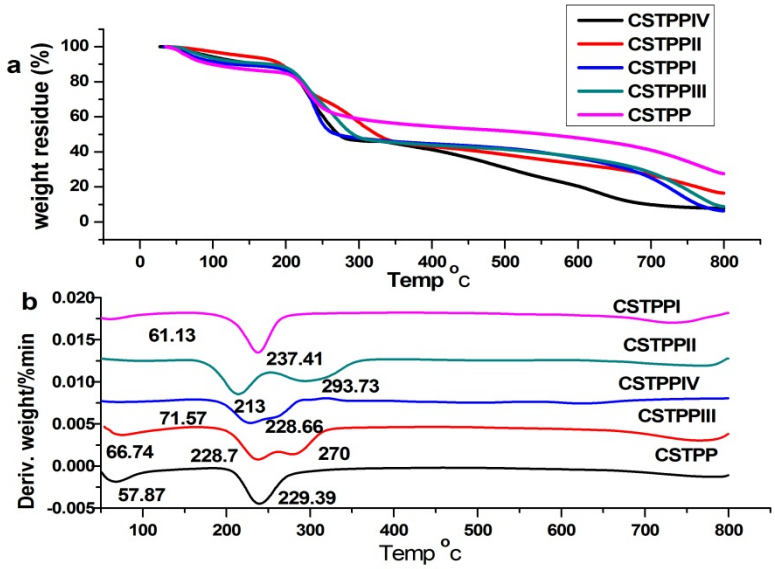

Fig 5: (a) TGA and (b) DTGA of CSTPP, CSTPPI, CSTPPII, CSTPPIII and CSTPPIV.

Table 1: Loading efficiency of quinazolinone derivatives onto CSTPP nanoparticles calculated using UV-Vis spectrophotometer and TGA.

Code	UV-Vis (Wt %)	TGA (Wt %)
CSTPPI	21.3	25
CSTPPII	23.7	21
CSTPPIII	20.2	13
CSTPPIV	16.3	18

Investigation of quinazolinone release kinetics and mechanism

Different mathematical models were applied for describing the kinetics of the release process of the quinazolinone derivatives, the most suited model being the one which best fits the experimental results was shown in Fig.7 and Fig.8. For each model the slope, regression coefficient R^2 and rate constant (k) are graphically determined and used to determine the kinetics mechanism of quinazolinone derivatives release.

The release rate constant $k_,$ k_1, k_H and k_{Hix} and k, release exponent value n and R^2 are summarized in table (2). Considering R^2 the release of (I-IV) in pH=6.8 from CSTPPI, CSTPPII, CSTPPIII and CSTPPIV follow Hixson-Crowell, Higuchi, zero orders and Krosmeyer-Peppas, respectively. Also release I-IV in pH=2 from CSTPPI, CSTPPII, CSTPPIII and CSTPPIV follow Krosmeyer-

Peppas, zero orders, Hixson-Crowell and first order. The value of release exponent n being between 0.56 and 1.2 given for CSTPPI, CSTPPII, CSTPPIII and CSTPPIV compounds (pH=2, 6.8) indicates that release follow non-Fickian diffusion processes.

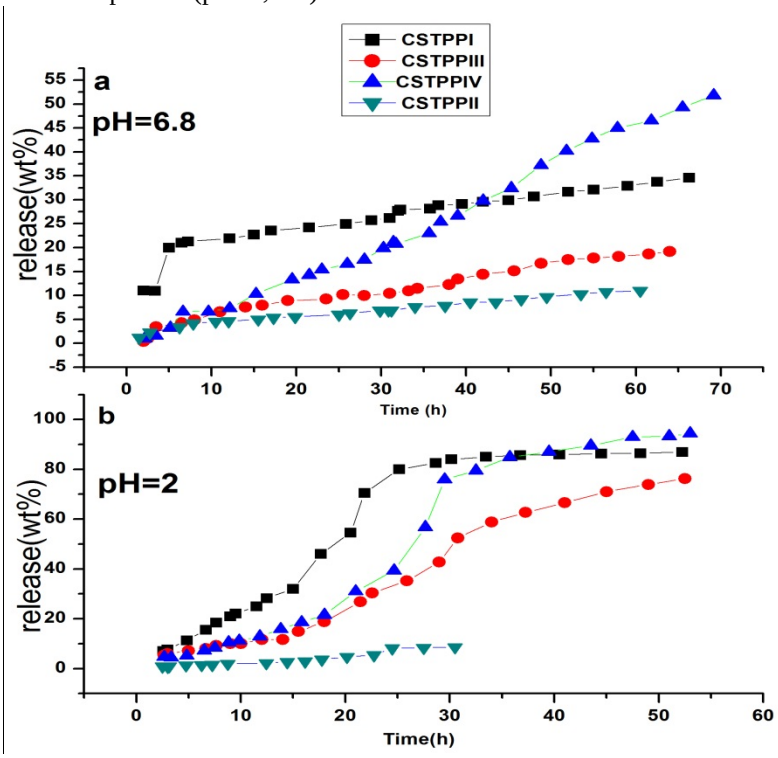

Fig 6: Release percent of I-IV from CSTPP nanoparticles at pH=6.8, 2.

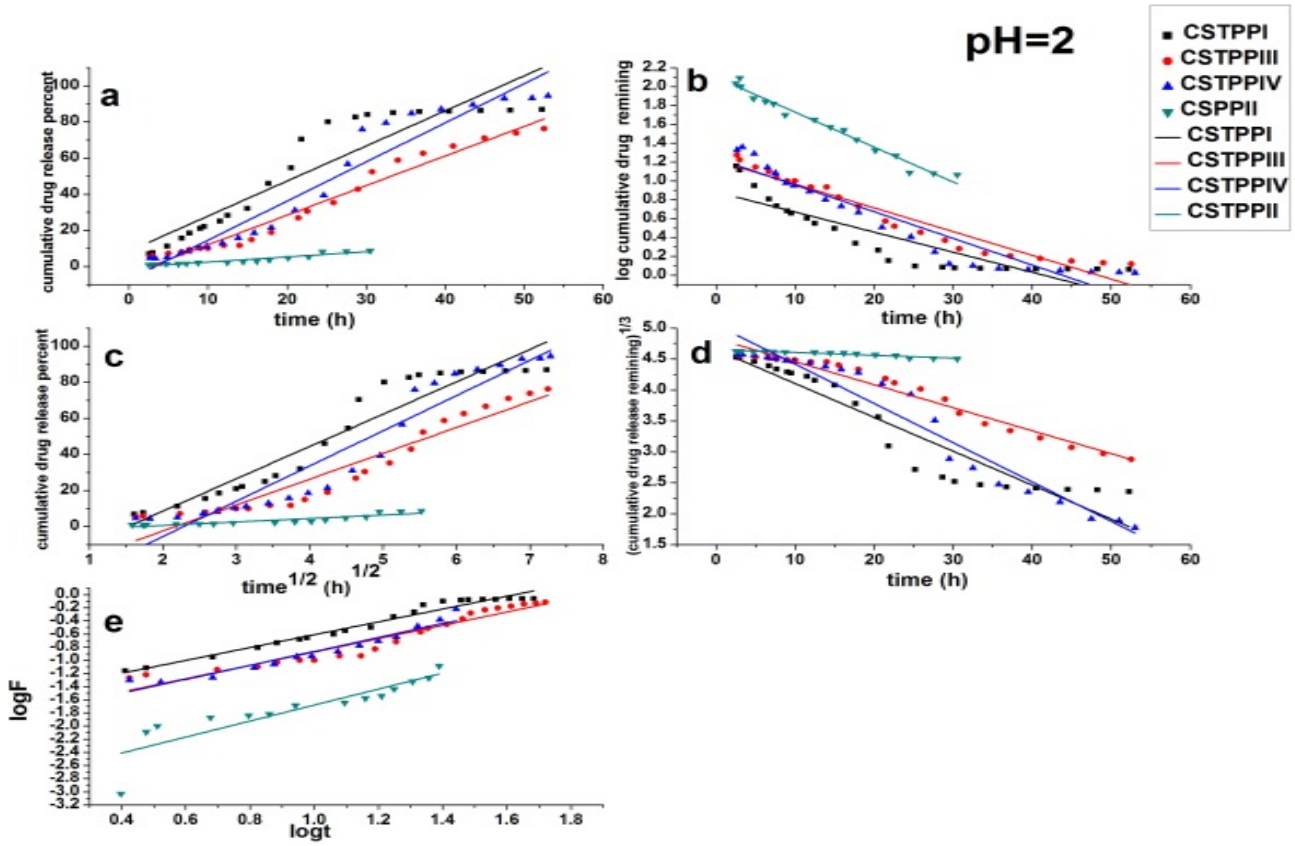

Fig 7: (a) Zero order, (b) First order, (c) Higuchi, (d) Hixson-Crowell and (e) Krosmeyer-Peppas kinetics of I- IV during time from CSTPP nanoparticles at pH=2.

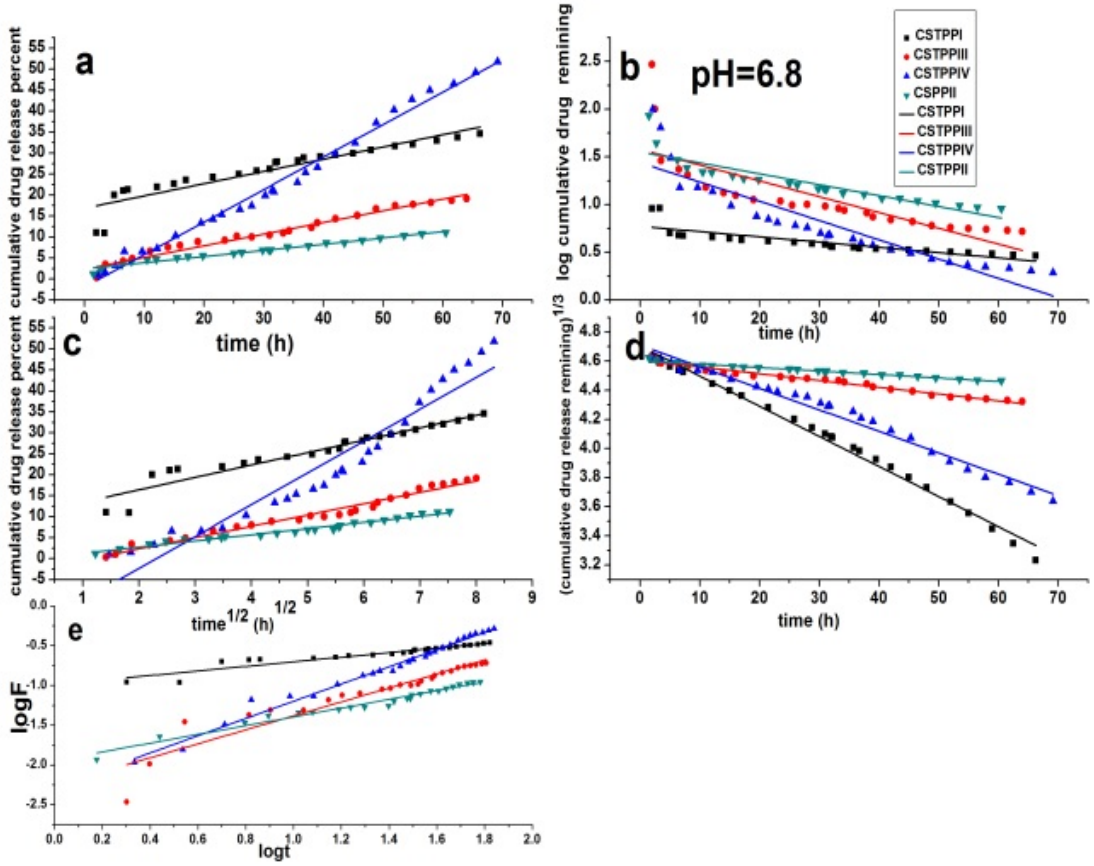

Fig 8: (a) Zero order, (b) First order, (c) Higuchi, (d) Hixson-Crowell and (e) Krosmeyer-Peppas kinetics of I-IV during time from CSTPP nanoparticles at pH=6.8.

Table 2: Controlled release kinetics of I, II, III and IV from CSTPP nanoparticles at pH=2, 6.8.

Code	pH	Zero order		First-order		Higuchi		Hixson-Crowell		Krosmeyer-Peppas		
		$k_{\circ}$	R^2	k_1	R^2	k_H	R^2	k_{Hix}	R^2	logk	R^2	n
CSTPPI	6.8	0.29163	0.8546	-0.00551	0.6958	2.96459	0.9212	-0.02069	0.98975	-0.989	0.895	0.56
	2	1.94012	0.8588	-0.2131	0.7647	17.92008	0.9169	-0.05479	0.8879	-1.586	0.97	0.9766
CSTPPII	6.8	0.14732	0.9691	-0.01145	0.6178	1.47751	0.9747	-0.00239	0.9732	-1.94	0.97	0.55
	2	0.28537	0.9679	-0.03708	0.9344	1.91611	0.9139	-0.00755	0.9611	-2.89	0.77	1.2
CSTPPIII	6.8	0.27821	0.9896	-0.01657	0.8103	2.69613	0.9261	-0.0465	0.9775	-2.26	0.8922	0.878
	2	1.63703	0.9377	-0.02519	0.8905	14.33851	0.9123	-0.03719	0.9466	-1.88	0.928	1.01
CSTPPIV	6.8	0.77341	0.9737	-0.02021	0.7826	7.59375	0.9745	-0.01478	0.9795	-2.282	0.983	1.08
	2	2.16512	0.9082	-0.02832	0.9745	19.51986	0.8245	-0.0635	0.9046	-1.9	0.9313	1.06

Antibacterial activity

To compare the antibacterial activity of quinazolinone derivatives and quinazolinone loaded on CSTPP nanoparticles the samples were tested against gram positive and gram negative bacteria. It is seen (Fig.9) that I-IV have a significant antibacterial activity against the tested microorganisms with variable inhibition zones expressed as mm. For E.coli, S.aureas this holds true regardless of the kind of bacterial used. In comparison with quinazolinone derivatives nanoparticles (CSTPPI, CSTPPII, CSTPPIII and CSTPPIV) were more active against the Gram negative bacteria (Escherichia coli) and Gram-positive bacteria (Staphylococcus aureus) than (I-VI), respectively as shown in Fig.9 although the percentage of the quinazolinone derivatives loaded on CSTPP nanoparticles was lower than 24% (Table. 1). This may be due to the small particle size [38]. The antibacterial activity of chitosan in acidic environment may result from its polycationic structure due to the protonation of $–NH_2^+$ on the C-2 position of the D-glucosamine. Positively charged chitosan can bind to bacterial cell surface which is negatively charged and disrupt the normal functions of the membrane, e.g. by promoting the leakage of intracellular components or by inhibiting the transport of nutrients into cells [39]. Phosphate ion reacts with Gram-positive by the same mechanism of CS without need to acid medium. In addition, quinazolinone derivatives have positively charge NH_3^+ that can also bind to negatively charged bacterial cell.

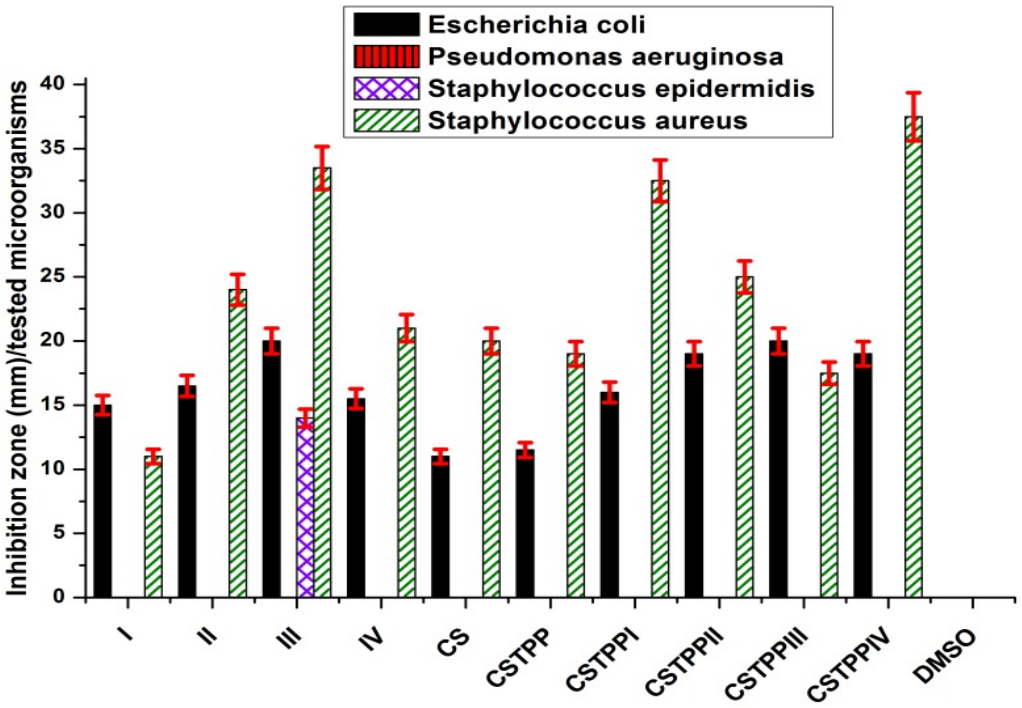

Fig 9: Antibacterial activities of I-IV, CSTPP, CSTPPI, CSTPPII, CSTPPIII and CSTPPIV.

Conclusion

The CS/Quinazolinone/TPP nanoparticles have been successfully prepared by mixing quinazolinone derivatives with CS followed by ionic gelation by TPP using ultrasonic waves. The loading efficiency was calculated by TGA and UV-Vis spectrophotometer. FT-IR spectra prove the interaction between quinazolinone derivatives and CSTPP nanoparticles. The synthesized nanoparticles CSTPP with average size of 21 nm were increased to 31-41 nm by loading of quinazolinone derivatives. The morphology of the nanoparticles is affected by substitutes on the quinazolinone. The in vitro release of loaded quinazolinone on CSTPP nanoparticles has been studied in two different pH media. According to Krosmeyer Peppas equation the release of quinazolinone derivatives followed anomalous non fickian diffusion. By applying the kinetics equations, the release (I-IV) in pH=6.8 from CSTPPI, CSTPPII, CSTPPIII and CSTPPIV follow Hixson-Crowell, Higuchi, zero orders and Krosmeyer-Peppas, respectively and at pH= 2 followed Krosmeyer-Peppas, zero orders, Hixson-Crowell and first order. In addition, quinazolinone loaded nanoparticles have better antibacterial activity in comparison with quinazolinone. The sustained release and the excellent antimicrobial activity suggest that the nanoparticles may serve as a promising therapy.

REFERENCES

[1] Raghavendra NM, Thampi PP, Gurubasavarajaswamy PM. Synthesis and Antimicrobial Activity of Some Novel Substituted Piperazinyl-quinazolin-3(4H)-ones, E-Journal of Chemistry 2008; 5:23-33.
[2] Alagarsamy V, Murugesan S, Dhanabal K, Murugan M, Clercq E. Anti HIV antibacterial and antifungal activities of some novel 2-methyl-3-(substituted methylamino)-(3H)-quinazolin-4-ones, Indian J Pharmaceut Sci 2007; 69:7-304.
[3] De la Fuente M, Csaba N, Garcia-Fuentes M, Alonso MJ. Nanoparticles as protein and gene carriers to mucosal surfaces, Nanomedicine 2008; 3: 845-857.
[4] Rawat M, Singh D, Saraf S. Nanocrriers: Promising vehicle for bio active drug, Biol pharm Bull 2006; 29: 1790-1798.
[5] Reis C, Ribeiro A, Neufeld R, Veiga F. Nanoencapsolation II. Biomedical appliceliers and current status of peptide and protein nanoparticle delivery systems, Nanomedicine: Nanotechnology, Biology, and Medicine 2006; 2: 53-65.
[6] Nagavarma BVN, Yadav H, Ayaz A, Vasudha LS, Shivakumar HG. Differenttechniques for preparation of polymeric nanoparticles- A review, Asian J Pharm Clin Res 2012; 5 (3): 16-32.
[7] Letchford K, Burt H. A review of the formation and classification of amphiphilic block copolymer nanoparticulate structures: micelles, nanospheres, nanocapsules and polymersomes, Eur. J. Pharm. Biopharm 2007; 65: 259–269
[8] Artusson P, Lindmark T, Davis SS and Ilium L. Effect of Chitosan on the Permeability of Monolayers of Intestinal Epithelial Cells (Caco-2), Pharmaceutical Research 1994; 11 (9): 1358-1361.
[9] Mi FL, Shyu S, Chen CT, Schoung JY. Porous chitosan microparticle for controlling the antigen release of Newcastle disease vaccine: preparation of antigen adsorbed microparticle and in vitro release, Biomaterials 1999; 20: 1603-1612.
[10] Bodmeier R, Oh K H, Pramar Y. Preparation and evaluation of drug-containing chitosan beads, Drug Dev Ind Pharm 1989; 15: 1475-1494.
[11] Harrise R, Panos I, Acosta N, Hears A. Preparation and chractrization of chitosan microshares for controlled release of tramadol, J Control Release 2008; 132 (3): 76-77.
[12] Sinha VR, Singla AK, Wadhawan S, Kaushik R, Kumria R, Bansal K, Dhawan S. Chitosan microspheres as potential carrier for drugs, Int J Pharmaceut 2004; 274: 1-33.
[13] Ganguli S, Panigrahi MK, Singh P, Shukla PK. One-pot synthesis of novel quinazolinone derivatives and their antimicrobial activity, Int J Pharm Pharm Sci 2012; 4 (4): 434-440.
[14] Varelas C, G Dixon, D G, Steiner C. Zero-order release from biphasic polymer hydrogels, J. Controlled Release. 1995; 34: 185-192.
[15] Kitazawa S, Johno I, Ito Y, Teramura S, Okada J. Effects of hardness on the desintegration time and the dissolution rate of uncoated caffeine tablets, J. Pharm. Pharmacol 1975; 27: 765-770.

[16] Hixson AW, Crowell JH. Dependence of reaction velocity upon surface and agitation, Ind. Eng. Chem 1931; 23: 923-931.
[17] Desai S, J Singh P, Simonelli AP, Higuchi WI. Investigation of factors influencing release of solid drug dispersed in inert matrices, III. Quantitative studies involving the polyethylene plastic matrix, J. Pharm. Sci 1966; 55: pp. 1230-1234.
[18] Korsmeyer RW, Gurny R, Doelker EM, Buri P, Peppas NA. Mechanism of solute release from porous hydrophilic polymers, Int J Pharmaceut 1983; 15:25-35.
[19] Ali SW, Rajendran S, Joshi M. Synthesis and characterization of chitosan and silver loaded chitosan nanoparticles for bioactive polyester, Carbohyd Polym 2011; 83: 438–446.
[20] Hosseinia SF, Zandib M, Rezaeia MR, Farahmandghavi F. Two-step method for encapsulation of oregano essential oil in chitosan nanoparticles: Preparation, characterization and in vitro release study, Carbohyd Polym 2013; 95: 50- 56.
[21] Yoksan R, Jirawutthiwongchai J, Arpo K. Encapsulation of ascorbylpalmitate in chitosan nanoparticles by oil-in-water emulsion and ionic gelation processes, Colloid Surface B 2010; 76: 292-297.
[22] Shivashankar M, Mandal BM, Uma K. Chitosan-acryl amide grafted polyethylene glycol interpenetrating polymeric network for controlled release studies of Cefotaxime, J Chem Pharm Res 2013; 5 (5): 140-146.
[23] Muhammed RPE, Junise V, Saraswathi R, krishnan PN, Dilip C. Development and characterization of chitosan nanoparticles loaded with isoniazid for the treatment of Tuberculosis, Res J Pharm Biol Chem Sci 2010; 1(4): 383-390
[24] Kafshgari MH, Khorram M, Khodadoost M, Khavari S. Reinforcement of Chitosan Nanoparticles obtained by an Ionic Cross-linking Process, Iran Polym J 2011; 20 (5): 445-456.
[25] Keawchaoon L, Yoksan R. Preparation characterization and in vitro release study of carvacrol-loaded chitosan nanoparticles, Colloid Surface B 2011; 84: 163–171.
[26] Kumar A, Harrison PM, Cheung KH, Lan N, Echols N, Bertone P, Miller P, Gerstein MB, Snyder M. An integrated approach for finding overlooked genes in yeast, Nat. Biotechnol 2002; 20(1): 58-63.
[27] Lima HA, Lia FMV, Ramdayal S. Preparation and characterization of Chitosan- Insulin- Tripoly phosphate Membrane for Controlled Drug Release Effect of Crosslinking agent, J Biomater Nanobiotechnol 2014; 5: 211-219.
[28] Lawrie G, Keen I, Drew B, Chandler-Temple A, Rintoul L, Fredericks P, Grøndahl L. Interactions between alginate and chitosan biopolymers characterized using FTIR and XPS, Biomacromolecules 2007; 8: 2533–2541.
[29] Zamora-Mora V, Fernández-Gutiérrez M, Román JS, Goya G, Hernández R, Mijangos C. Magnetic core–shell chitosan nanoparticles: Rheological characterization and hyperthermia application, Carbohyd Polym 2014;102: 691- 698.
[30] Jingou J, Shilei H, Weiqi L, Danjun W, Tengfei W, Yi X. Preparation characterization of hydrophilic and hydrophobic drug in combine loaded chitosan cyclodextrin nanoparticles and in vitro release study, Colloid Surface B 2011; 83:103-107.
[31] Rodrigues S, Costa AMR, Grenha A. Chitosan/carrageenan nanoparticles: Effect of cross-linking with tripolyphosphate and charge ratios, Carbohyd Polym 2012; 89: 282–289.
[32] Gao X, Cai X, Yan K, Song B, Gao L, Chen Z. Synthesis and Antiviral Bioactivities of 2-Aryl- or 2-Methyl-3-(substituted- Benzalamino)-4(3H)-quinazolinone Derivatives, Molecules 2007; 12: 2621-2642
[33] Bhumkar DR, Pokharkar VB. Studies on Effect of pH on Cross-linking of Chitosan with Sodium Tripolyphosphate, AAPS Pharm Sci Tech 2006; 7 (2): 138-143.
[34] Orienti I, Aiedeh K, Gianasi E, Bertasi V; Zecchi V. Indomethacin loaded chitosan microspheres. Correlation between the erosion process and release kinetics, J Microencapsul 1996; 13: 463– 472
[35] Zhou S, Deng X, Li X. Investigation on anovel cor- coated microsphares protein delivery system, J Control Release 2001; 75: 27-36.
[36] Wu Y, Yang W, Wang C, Hu J, Fu S. Chitosan nanoparticles as novel delivery system for ammonium glycyrrhizinate, Int J Pharmaceut 2005; 295: 205-235.
[37] Chen F, Zhang ZR, Huang Y. Evaluation and modification of N-tri methyl chitosan chloride nanoparticles as protein carriers, Int J Pharmaceut 2007; 336:166-173.
[38] Zhang L, Jiang Y, Ding Y, Povey M, York D. Investigation into the antibacterial behavior of suspensions of ZnO nanoparticles (ZnO nanofluids), J Nanopart Res 2007; 9: 479-489.
[39] Helander IM, Nurmiaho-Lassila E-L, Ahvenainen R, Rhoades J, Roller S. Chitosan disrupts the barrier properties of the outer membrane of Gram-negative bacteria, Int J Food Microbiol 2001; 71: 235–244.

AUTHORS

First Author – Nehal Salahuddin, professor, Department of Chemistry, Faculty of Science, Tanta University, Tanta, E-mail: nehal.attaf@science.tanta.edu.eg, salahuddin.nehal@yahoo.com.
Second Author – Ahmed A. Elbarbary, professor, Department of Chemistry, Faculty of Science, Tanta University, Tanta, E-mail: aeelbarbary@hotmail.com.
Third Author – Hend A. Alkabes, Department of Chemistry, Faculty of Science, Tanta University, Tanta, E-mail: hendelkabes@hotmail.com.

*Correspondence Author – Nehal Salahuddin, professor, Department of Chemistry, Faculty of Science, Tanta University, Tanta, E-mail: nehal.attaf@science.tanta.edu.eg.